IU-NTC-92-12

IU/NTC 92-12

April, 1992

Fermilab Library
0 1160 0015541 0

Density Dependence of Nuclear Neutrino Pair Production

C. J. Horowitz
Nuclear Theory Center, Indiana University
2401 Milo B. Sampson Lane, Bloomington, Indiana 47405

FERMILAB
MAY 15 1992
LIBRARY

ABSTRACT

Nuclear decay via neutrino pair production is found to have a large density dependence because of intermediate electromagnetic couplings to electrons. These are calculated in a relativistic random phase approximation. The decay rate for vector (Fermi) transitions producing electron type neutrino pairs can be enhanced by 10^5 or more at densities relevant for stellar collapse.

ROUTE TO
NAME
LOCATION
LIBRARY

I. Introduction.

A variety of weak neutral current reactions are of interest in astrophysics. For example, neutrino-nucleus elastic scattering influences neutrino transport in a supernova. Neutral current reactions may have a large density dependence because of matter induced Z^0 photon mixing. Indeed, this mixing was found to strongly reduce neutrino-nucleus elastic cross sections [1,2].

In this letter, we examine the density dependence of nuclear decay via neutrino pair production. These reactions have been considered by Fuller et.al. [3] and are interesting for supernovas because the neutrino pairs can transport energy without carrying net lepton number (in contrast to neutrinos produced in charged current reactions).

The density dependence of conventional beta decay (from Pauli blocking of the outgoing electron) is well known. Here, we consider an intermediate coupling of the nucleus to a particle-hole excitation of the dense relativistic electron gas which then couples to a neutrino pair (see Fig. 1). This coupling will be important for kinematics near the plasmon or transverse photon collective modes and can lead to a large increase in the decay rate.

In general, the coupled system of neutrinos interacting with a dense electron gas is a non-trivial example of a relativistic many-body problem. The relativistic many-body problem is interesting. For example, there is mixing between particle-hole and particle-antiparticle excitations. By studying this simple, weakly interacting, system one may gain useful insight for strongly interacting systems such as the QCD plasma.

II. Formalism

In this paper we calculate how correlations involving the dense electron gas change the basic decay rate of Fig. (1a). In order to separate the electron and nuclear physics, we will calculate a ratio of the total decay rate to the decay rate ignoring the electron contributions. This ratio will be used in a later work, along with a model of the nuclear transition strength, to calculate the total neutrino production rate.

The rate of nuclear decay via pair production ω for the original diagram in Fig. (1a) is easily calculated. This has contributions from both axial-vector (Gamow-Teller) and vector (Fermi) weak neutral currents. Only the vector neutral current will be modified by the coupling to electrons. Therefore, in what follows, *we assume a pure vector transition. The axial-vector contribution to the decay rate will be unchanged.*

The vector transition rate is easily calculated,

$$\omega \sim \int \frac{d^3p d^3l}{p_0 l_0}[2(p\cdot J)(l\cdot J) - (p\cdot l)(J\cdot J)]\delta(p_0 + l_0 - q_0). \tag{1}$$

Here p is the momentum of the neutrino and l the momentum of the antineutrino. For a longitudinal transition, the nuclear current J_μ has zero J_0 and longitudinal

J_1 components related by current conservation $q \cdot J = 0$. We adopt a frame where the one axis is along the momentum transfer $\vec{q} = \vec{p} + \vec{l}$. The energy of the nuclear transition is q_0. For a transverse transition, $J_0 = 0$.

For simplicity, we assume first forbidden transitions so that,

$$J_0 = q\rho, \qquad \text{Longitudinal} \tag{2}$$

$$J_2 = J_3 = qj_t, \qquad \text{Transverse} \tag{3}$$

with $q = |\vec{q}|$. Note, Ref. [3] showed that there is considerable first forbidden strength. Higher forbidden transitions will give similar results.

Using Eqs. (2-3), Eq. (1) is easily integrated. For longitudinal transitions the decay rate is proportional to the phase space integral,

$$\omega_l^0 = \int_0^{q_0} dq f_l(q, q_0) = \frac{8}{135} q_0^7, \tag{4}$$

$$f_l(q, q_0) = q_\mu^4 q^2. \tag{5}$$

While the transverse phase space integral is,

$$\omega_t^0 = \int_0^{q_0} dq f_t(q, q_0) = \frac{2}{35} q_0^7, \tag{6}$$

$$f_t(q, q_0) = q_\mu^2 q^4. \tag{7}$$

It is now a simple matter to modify these phase space integrals to include other diagrams.

The response of the dense relativistic electron gas can be included in a relativistic random phase approximation (RPA). This includes all the ring diagrams of Figs. (1a and b) and is expected to be an excellent approximation at the high densities appropriate for stellar collapse. The ratio of the transition matrix element squared for the sum of all diagrams in Fig. 1 to the bare nuclear process (Fig. 1a only) is easily calculated,

$$r(q, q_0) = \left|1 + (1 - \frac{1}{\epsilon(q, q_0)})g\right|^2. \tag{8}$$

Here $\epsilon(q, q_0)$ is either the longitudinal ϵ_l or transverse ϵ_t dielectric function of the electron gas depending on the nuclear transition. These functions are given in Ref. [4],

$$\epsilon_l(q, q_0) = 1 + \frac{e^2}{q_\mu^2} \Pi_l(q, q_0), \tag{9}$$

$$\epsilon_t(q, q_0) = 1 - \frac{e^2}{q_\mu^2} \Pi_t(q, q_0), \tag{10}$$

where e is the electric charge and the relativistic polarizations Π_i are calculated analytically at zero temperature [4].

Finally, g is the ratio of the weak charge of the electron c_v^e, to that of a nucleon C_v^N,

$$g = c_v^e / C_v^N. \tag{11}$$

The electron's charge is,

$$c_v^e = 2\sin^2(\theta_w) \pm \frac{1}{2}, \tag{12}$$

with the plus sign for electron neutrino pairs and the minus sign for the production of mu or tau neutrino pairs. [We use a Weinberg angle $\sin^2(\theta_w) = 0.223$.] For simplicity we assume a nuclear electromagnetic current that is a sum over nucleons,

$$J_\mu^{em} = \sum_i -e\gamma_{\mu i}[\frac{1+\tau_{3i}}{2}], \tag{13}$$

and a weak vector current,

$$J_\mu = \sum_i \gamma_{\mu i}([\frac{1}{2} - 2\sin^2(\theta_w)][\frac{1+\tau_{3i}}{2}] - \frac{1}{2}[\frac{1-\tau_{3i}}{2}]). \tag{14}$$

Thus C_v^N for an isoscalar transition is,

$$C_v^N = -2\sin^2(\theta_w), \tag{15}$$

and for an isovector transition,

$$C_v^N = 1 - 2\sin^2(\theta_w). \tag{16}$$

Thus g is 1.708 (-2.121) for an isovector (isoscalar) transition producing electron type neutrino pairs and -0.098 (+0.121) for the production of muon or tau neutrinos.

The ratio of total decay rates is obtained by integrating Eq. (8) over the phase space in Eqs. (4-7). This gives,

$$< r >_t = \frac{1}{\omega_t^0} \int_0^{q_0} dq f_t(q, q_0) |1 + (1 - \frac{1}{\epsilon_t})g|^2, \tag{17}$$

$$< r >_l = \frac{1}{\omega_l^0} \int_0^{q_0} dq f_l(q, q_0) |1 + (1 - \frac{1}{\epsilon_l})g|^2. \tag{18}$$

These simple expressions are the basic results of this paper and describe how the electron medium modifies the neutral current decay rate.

Often the integrals in Eqs. (17-18) are dominated by the transverse photon or longitudinal plasmon collective modes where,

$$\mathrm{Re}\,\epsilon(q_c, q_0) = 0. \tag{19}$$

The dispersion relations q_0 as a function of q_c implied by Eq. (19) are discussed in Ref. [5]. If one expands the dielectric function for q near q_c,

$$\epsilon(q, q_0) \approx (q - q_c)\beta + i\epsilon_i, \tag{20}$$

the integrals (Eqs. 17, 18) can be easily evaluated, for example,

$$< r >_t \approx \frac{\pi g^2}{\omega_t^0 |\beta \epsilon_i|} f_t(q_c, q_0). \tag{21}$$

This shows that the rate depends on the imaginary part of the dielectric function (ϵ_i).

A collective mode can decay into an electron-positron pair or into a two particle-two hole excitation. Decay into a single particle-hole excitation is not possible for these time-like momentum transfers $q_0 > q$. Electron-positron decay is Pauli blocked at zero temperature for q_0 much less then the Fermi energy [6]. Thus 2p-2h decay probably dominates the width. However, e^+e^- can contribute at high temperatures (see below).

Unfortunately, we are not aware of a relativistic calculation of the 2p-2h width. Therefore, we make a crude estimate based on a nonrelativistic calculation. Glick and Lang [7] estimate the 2p-2h contribution to ϵ_i for the longitudinal mode for q_c much less than the Fermi momentum (k_F) to be,

$$|\epsilon_i| = \alpha(\frac{q_c}{k_F})^2. \tag{22}$$

Here, the coefficient α is predicted to depend only weakly on density. Perhaps the highest density at which the nonrelativistic calculation can be directly applied is $k_F = m$ with m the electron mass. At this density the analytic estimate (including Thomas-Fermi screening) gives $\alpha = 0.13$ [7]. For higher densities, Glick and Lang predict that α will change only very slowly with density as $\rho^{-1/12}$ (and that screening will be unimportant). Therefore, we simply take,

$$\alpha \approx 0.1, \tag{23}$$

for all the densities of interest here. As a further crude approximation, we will use Eqs. (22) and (23) also for transverse modes. [Note, at small q the dispersion relation for the transverse mode is very close to that for the longitudinal plasmon.]

It is hoped that Eqs. (22-23) will allow us to make an order of magnitude estimate of the enhancement of the neutrino rate. If ϵ_i is significantly different from Eqs. (22-23), then Eq. (21) shows that the enhancement factor will scale with one over ϵ_i.

III. Results

The ratio of transition rates is plotted in Fig. 2 for longitudinal transitions at a density of $9.1/Y_e$ x 10^{11} (g/cc). Here Y_e is the electron to baryon ratio. This

corresponds to an electron Fermi momentum of 50 MeV. Note, Eq. (18) has been numerically integrated rather then simply using Eq. (21).

The ratio can be as large as 10^6 or more for the production of ν_e pairs. The ratio for ν_τ or ν_μ pairs is much smaller because of the small value of c_v^e in Eq. (12). The ratio rapidly increases at the plasma frequency $q_0 \approx 2.8$ MeV. Just above this frequency, q_c is small, so the damping in Eq. (22) is also small, this gives a large enhancement. As the energy increases further, the dispersion relation for the plasmon rapidly becomes light-like, $q_0^2 - q_c^2 \to 0$. Therefore, the phase space factor in Eq. (5) causes the ratio to rapidly decrease.

Near the peak, the ratio is similar for isoscalar and isovector transitions. However, these have different interference terms which show up at low and high energies. The Z^0 couples primarily to neutrons (see Eq. (14) with $\sin^2(\theta_w) \approx 1/4$) while the photon couples to protons. Therefore, the relative phase of the interference term changes with isospin.

The ratio for transverse transitions, Eq. (17), is shown in Fig. (3). This can be as large as 10^5. The transverse dispersion relation does not have $q_0^2 - q_c^2 \to 0$ nearly as fast. Furthermore, the phase space factor in Eq. (7) is different. Therefore, the transverse ratio is enhanced at higher energies than the longitudinal. [Note, the eventual fall off in the ratio at high energy may be sensitive to our assumption for the width in Eq. (22) which becomes large for large q_c.]

For muon or tau neutrino pairs there is again only a modest enhancement. Note, for transverse transitions, there is a small mixing term between vector and axial-vector currents (proportional to the Π_{va} of Ref. [4]) which allows the axial coupling of the electrons to contribute. This term (which we neglect) is very small for electron neutrinos but could be about a 10 percent correction for mu or tau neutrinos.

The magnitude of the enhancement is similar at other densities. However, the enhancement affects lower energies as the density decreases. Fig. (4) plots (as a solid line) the plasma frequency vs. density. Excitations with smaller energies will not be significantly enhanced. Also shown in Fig. (4) (as a dotted line) is the upper energy where $< r >_l = 10$. Longitudinal transitions with energies between these solid and dotted lines will be significantly enhanced. Finally, the dashed line in Fig. (4) is the upper energy where $< r >_t = 10$. Transverse transitions in this larger energy range between the dashed and solid lines will be significantly enhanced.

Our calculations have been for zero temperature. However, we do not expect a strong temperature dependence as long as the system is still degenerate. At a temperature of 15 MeV, there is a small contribution to the plasmon width from e^+e^- decay, which we calculate as in Refs. [8-9]. This leads to a small decrease in the peak of $< r >_l$ in Fig. (2). To investigate nondegenerate conditions, one will need a finite temperature calculation of the 2p-2h decay width.

IV. Summary

We have calculated the density dependence of the nuclear decay rate to neu-

trino pairs. This arises because of an intermediate coupling to electron particle-hole excitations. We treated the dense electron gas in a relativistic RPA and used a crude nonrelativistic estimate of collective mode widths from 2p-2h excitations.

The transition rates can be greatly enhanced. Furthermore, transverse modes are enhanced over a larger energy range than longitudinal modes. However, only vector (Fermi) transitions to electron type neutrino pairs are significantly enhanced. We will use these enhancement factors, Eqs. (17-18), along with a model of the nuclear transition strength in a later work to calculate the total neutrino production rate.

Acknowledgement

This work was supported in part by DOE grant DE-FG02-87ER40365.

References

1. C.J. Horowitz and K. Wehrberger, Phys. Rev. Lett. **66** (1991) 272.
2. L.B. Leinson, V.N. Oraevsky and V.B. Semikoz, Phys. Lett. **B209** (1988) 80.
3. George M. Fuller and Bradley S. Meyer, Astro. Phys. J **376** (1991) 701.
4. C.J. Horowitz and K. Wehrberger, Nucl. Phys. **A531** (1991) 665.
5. Eric Braaten, Phys. Rev. Lett. **66** (1991) 1655.
6. S. Chin, Ann. of Phys. (NY) **108** (1977) 301.
7. A.J. Glick and W.F. Lang, Phys. Rev. **B4** (1971) 3455.
8. C.J. Horowitz and K. Wehrberger, Phys. Lett. **B266** (1991) 236.
9. K. Saito, T. Maruyama and K. Soutame, Phys. Rev. **C40** (1989) 407.

Figure Captions

Figure 1. (a) Nuclear decay via emission of a Z^0 which produces a neutrino pair. (b) Nuclear decay via intermediate electromagnetic couplings to electron particle-hole excitations.

Figure 2. Ratio of decay rate at a density (times electron fraction Y_e) of $9.1\times10^{11}(g/cc)$ to that in free space for a longitudinal transition to ν_e pairs, see Eq. (18). The solid (dot-dashed) curve is for an isoscalar (isovector) transition. The dotted curve is for the production of ν_μ or ν_τ pairs in an isovector transition.

Figure 3. As per Fig. 2 except for transverse transitions, see Eq. (17).

Figure 4. Plasma frequency (solid curve) vs. density (times electron fraction Y_e). Also shown is the upper energy where $< r >_l = 10$, Eq. (18) (dotted) and $< r >_t = 10$ (dashed curve). Transverse transitions are significantly enhanced for energies between the dashed and solid curves, while longitudinal transitions are enhanced for energies between the dotted and solid curves.

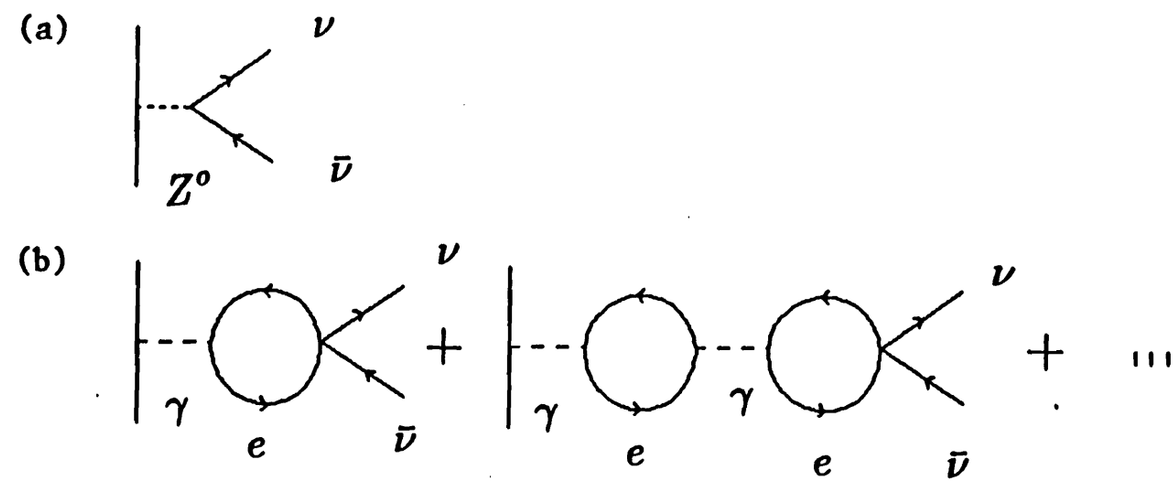

Fig. 1

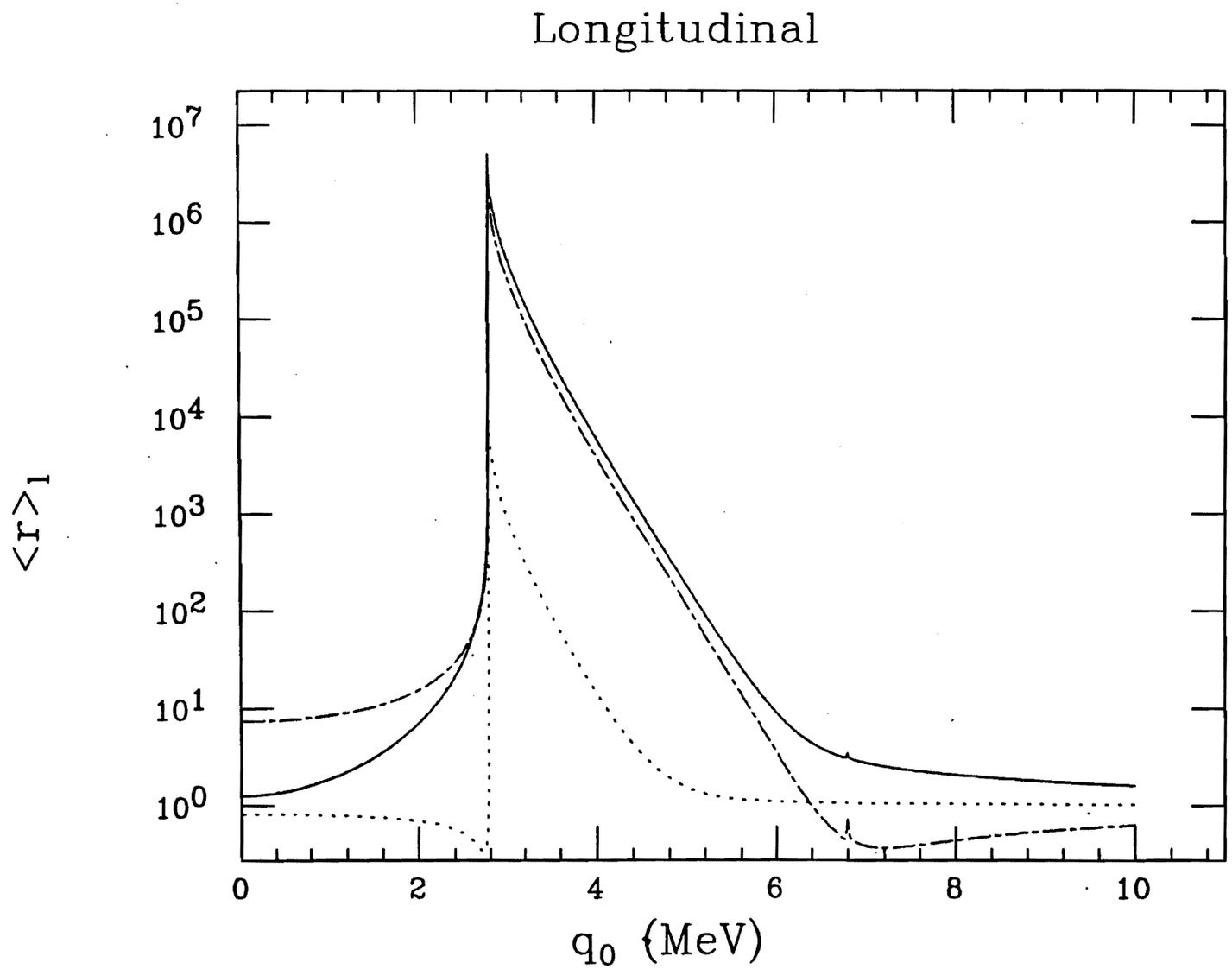
Longitudinal
10^7
10^6
10^5
10^4
10^3
10^2
10^1
10^0
$\langle r \rangle_l$
0
2
4
6
8
10
q_0 (MeV)

Fig. 2

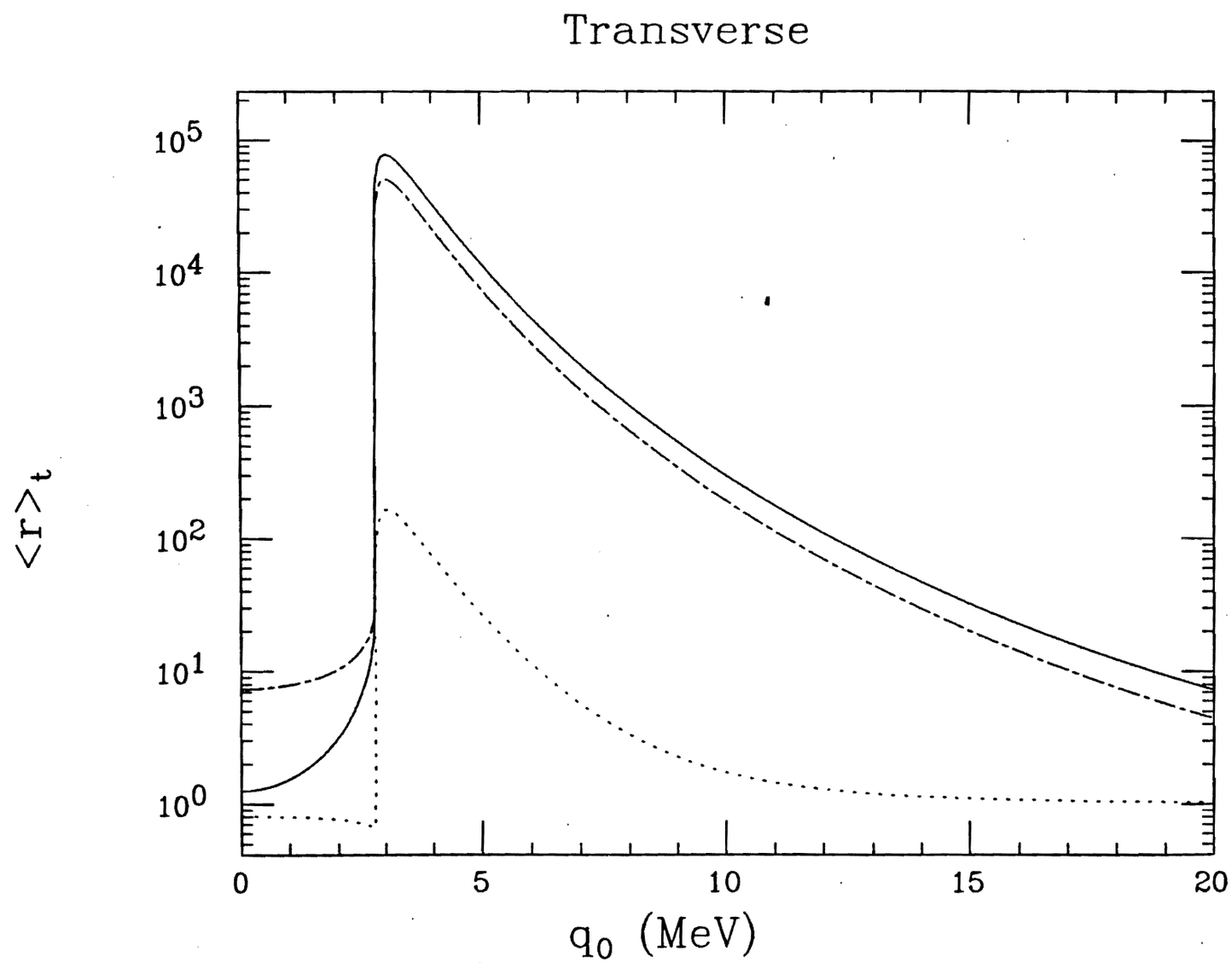
Transverse
10^5
10^4
10^3
10^2
10^1
10^0
$\langle r \rangle_t$
0
5
10
15
20
q_0 (MeV)

Fig. 3

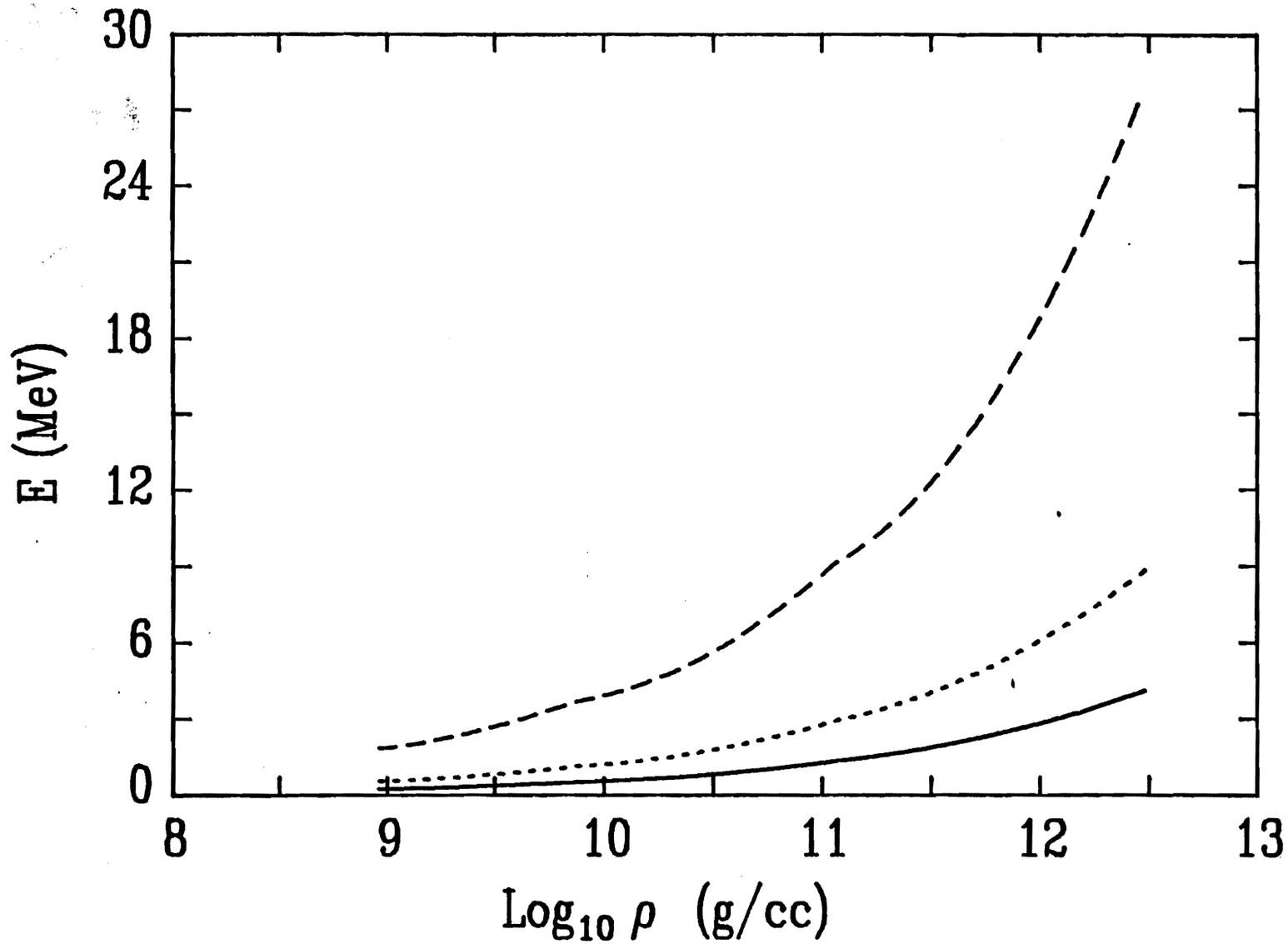

Fig. 4